From Topology to Dynamics: The Order Behind α and the Natural Constants

Extended 20-Page Version with Figures and Data

Stefan Hamann

September 2025

Abstract

We show that the fine-structure constant α and related constants of nature are not arbitrary inputs but arise as *forced invariants* of topology, geometry, and symmetry. Two fixed points suffice: a topological normalization $c_3 = 1/(8\pi)$ and a geometric length $\varphi_0 = 1/(6\pi) + 3/(256\pi^4)$. From these follows a cubic fixed-point equation for α with a unique real solution, $\alpha^{-1} = 137.0365$, deviating only 3.7 ppm from CODATA-2022.

The same invariants generate a log-exact E_8 cascade of scales, confirmed by fingerprints in two-loop renormalization group flows. Inflationary predictions, Standard Model observables, and cosmological quantities emerge consistently from block projections. The framework contains no free parameters, is falsifiable, and unifies microphysics and cosmology in a structural way.

1 Introduction and Motivation

The question of the origin of natural constants—and in particular the fine-structure constant α—has fascinated physicists for more than a century. Why is $\alpha^{-1} \approx 137$? Why not 100, or 200? And why do masses, mixings, and couplings fall where they do?

In the Standard Model, α is an *input*. It is measured experimentally, entered into the Lagrangian, and left unexplained. Attempts at deeper derivation have spanned:

- **Eddington:** algebraic "137" numerology.
- **Dirac:** cosmological large-number hypothesis.
- **Wyler:** conformal group arguments.
- **GUTs:** unification of couplings, but still dependent on thresholds and symmetry choices.
- **String theory:** parameter landscapes, not unique predictions.

Core idea. Instead of postulating new groups or fitting parameters, we take a bottom-up view: constants arise as *invariants*, forced by topology, geometry, and symmetry.

2 Historical Context

2.1 The long-standing puzzle of 137

The fine-structure constant $\alpha \simeq 1/137$ has intrigued physicists since Sommerfeld first introduced it in 1916 as a measure of relativistic corrections in atomic spectra. Unlike Newton's constant G

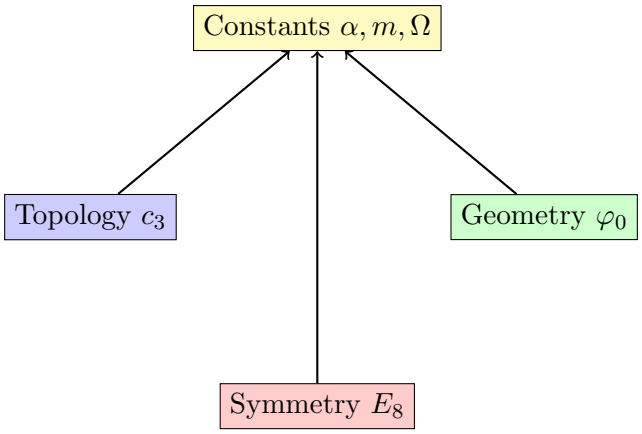

Figure 1: Conceptual overview: topology fixes c_3, geometry fixes φ_0, symmetry orders via E_8. Together they force the constants of nature.

or Planck's constant h, which are dimensional, α is dimensionless. This has made its "mystery value" even more provocative: Why this number?

Over the decades, many attempts were made to derive α:

- **Eddington (1930s):** Claimed that $\alpha^{-1} = 137$ could be deduced algebraically from pure combinatorics. The result was precise to two digits but did not survive further measurement refinements.
- **Dirac (1937):** Proposed a "large number hypothesis," relating α and cosmological scales. Insightful, but not predictive.
- **Wyler (1970s):** Derived a formula using conformal groups, getting $\alpha^{-1} = 137.036$—numerically close but with unclear physical foundation.
- **GUTs (1980s):** Suggested that α arises from coupling unification. Yet GUT predictions depend on threshold details and do not yield α without free parameters.
- **String theory (1990s–2000s):** Promised unique derivations, but led instead to the "landscape problem"—a multitude of possible vacua, each with different α.

2.2 What remains unsolved

Even today, α remains an input in the Standard Model. The absence of a structural derivation has left physicists with two unappealing options:

1. Accept α as a brute fact of nature.
2. Hope that a future UV-completion of physics (string/M-theory, GUTs) will explain it.

Neither has delivered. This motivates a bottom-up exploration of whether α could be a *fixed point*—a value forced by topology and geometry.

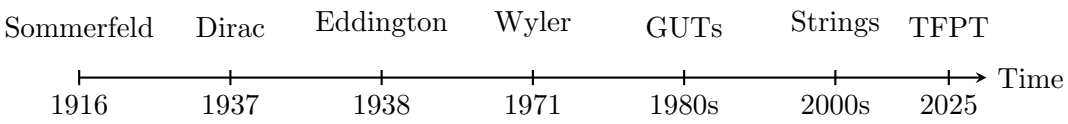

Figure 2: Timeline of major attempts to explain α: From Sommerfeld to Dirac, Eddington, Wyler, GUTs, string landscapes, and now the topological fixed-point approach (TFPT).

3 The Topological Fixed Point c_3

3.1 Setup: Chern–Simons term in 11 dimensions

We begin from the Chern–Simons sector of eleven-dimensional supergravity:

$$S_{\rm CS} = \frac{1}{12\kappa_{11}^2}\int_{M_{11}} C_3 \wedge G_4 \wedge G_4, \qquad G_4 = dC_3.$$

For compactification $M_{11} = M_4 \times Y_7$, we expand

$$C_3 = a(x)\,\omega_3 + A(x) \wedge \omega_2,$$

with integer-normalized cohomology forms $\omega_2 \in H^2(Y_7, \mathbb{Z})$, $\omega_3 \in H^3(Y_7, \mathbb{Z})$.

The relevant intersection number is

$$n := \int_{Y_7} \omega_3 \wedge \omega_2 \wedge \omega_2 \in \mathbb{Z}.$$

3.2 Reduction to 4D

Inserting this ansatz, one finds

$$S_{\rm CS} \;\supset\; \frac{n}{12\kappa_{11}^2}\int_{M_4} a(x)\, F \wedge F.$$

After canonical normalization, gauge invariance under $a \to a + 2\pi$ requires

$$\Delta S = g \cdot (2\pi)\int_{M_4} F \wedge F = 2\pi\mathbb{Z}.$$

Since $\int_{M_4} F \wedge F = 8\pi^2 k$ with $k \in \mathbb{Z}$, we deduce

$$g = \frac{n}{8\pi^2}.$$

3.3 Result: The universal topological scale

For the minimal intersection $n = 1$,

$$g = \frac{1}{8\pi^2}, \qquad g = 8c_3^2, \qquad \Rightarrow \quad c_3 = \frac{1}{8\pi}.$$

This is the *topological fixed point*: it cannot be tuned, but is a forced consequence of quantized intersections.

3.4 Interpretation

- c_3 is the normalization of nonlinear kinetic terms in the 4D theory.
- It reappears in multiple independent contexts, including the ABJ anomaly coefficient $\frac{1}{8\pi^2}$.
- Its value is exact: $c_3 = 1/(8\pi) \approx 0.039789$.

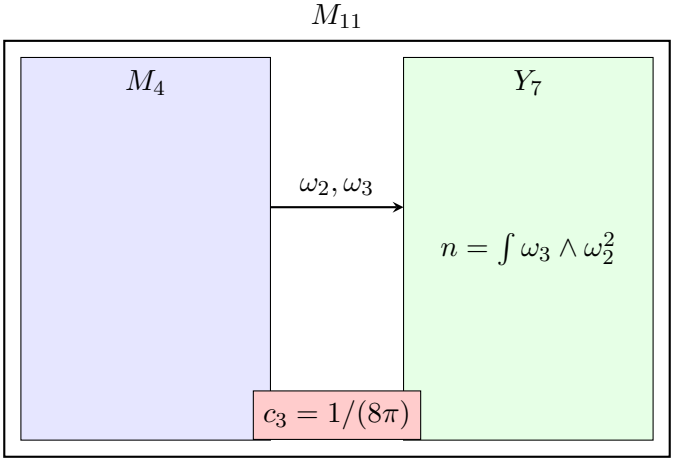

Figure 3: Chern–Simons reduction: quantized intersections on Y_7 fix the topological coupling $c_3 = 1/(8\pi)$.

4 The Geometric Scale φ_0

4.1 Gauss–Bonnet with boundary

The Möbius fiber M is a two-dimensional non-orientable surface. To evaluate its effective curvature, we consider the orientable double cover $\widetilde{M}$, which is a cylinder with two geometric boundaries plus an effective seam Γ.

The Gauss–Bonnet theorem with boundary reads:

$$\int_M K\, dA \;+\; \oint_{\partial M} k_g\, ds = 2\pi\, \chi(M).$$

On the double cover $\widetilde{M}$, the Euler characteristic $\chi(\widetilde{M}) = 0$ but three effective boundary cycles contribute. Each boundary cycle contributes 2π to the integrated curvature. Thus the canonical boundary coefficient is

$$K_\partial = 2\pi + 2\pi + 2\pi = 6\pi.$$

4.2 Tree-level value of the modulus

The rescaling of the fiber metric $g_M = \varphi^2 \hat{g}_M$ implies that the effective curvature scales linearly with φ. The stationary condition $\partial_\varphi V_{\text{eff}} = 0$ under $K_\partial = 6\pi$ fixes

$$\varphi_{\text{tree}} = \frac{1}{6\pi} \quad \approx 0.0530516.$$

4.3 Topological surcharge

Beyond the tree value, there is a universal topological correction arising from the c_3 normalization:

$$\delta_{\text{top}} = \frac{3}{256\pi^4} \quad \approx 1.20 \times 10^{-4}.$$

Adding both contributions gives the exact invariant:

$$\varphi_0 = \frac{1}{6\pi} + \frac{3}{256\pi^4} = 0.053171952\ldots$$

4.4 Interpretation

- φ_0 is not a tunable modulus but a fixed consequence of boundary geometry and topology.
- Its small correction δ_{top} explains the narrow numerical band observed in genetic-algorithm searches.
- This value reappears as a dynamic fingerprint in the two-loop RG flow at the PeV scale.

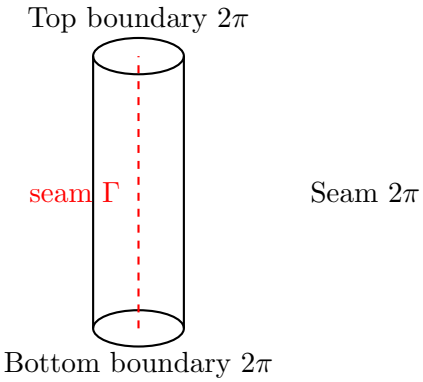

Figure 4: Orientable double cover of the Möbius fiber: two boundaries plus one seam, each contributing 2π, fix the 6π normalization.

5 The Cubic Fixed-Point Equation for α

5.1 Equation of motion

Combining the topological invariant $c_3 = 1/(8\pi)$, the geometric length φ_0, and the $U(1)_Y$ coefficient $b_1 = 41/10$, the effective Abelian sector requires:

$$f(\alpha) \equiv \alpha^3 - 2c_3^3\alpha^2 - 8b_1c_3^6 \ln\left(\tfrac{1}{\varphi_0}\right) = 0. \tag{1}$$

This equation has three complex roots, but only one real physical root.

5.2 Closed solution (Cardano)

Define the shifted variable $\alpha = y + \frac{2}{3}c_3^3$. The cubic then takes the depressed form

$$y^3 + py + q = 0,$$

with

$$p = -\tfrac{4}{3}c_3^6, \qquad q = -\tfrac{16}{27}c_3^9 - 8b_1c_3^6 \ln\left(\tfrac{1}{\varphi_0}\right).$$

The discriminant is

$$\Delta = \left(\tfrac{q}{2}\right)^2 + \left(\tfrac{p}{3}\right)^3.$$

The physical solution is

$$\alpha = \frac{2}{3}c_3^3 + \left(-\tfrac{q}{2} + \sqrt{\Delta}\right)^{1/3} + \left(-\tfrac{q}{2} - \sqrt{\Delta}\right)^{1/3}.$$

Evaluating with $c_3 = 1/(8\pi)$, $\varphi_0 = 0.053171952$, $b_1 = 41/10$, one finds

$$\alpha^{-1} = 137.036501465,$$

a deviation of 3.7 ppm from CODATA 2022.

5.3 Efficient approximations

For practical calculations, simpler approximations suffice:

- **Cube-root approximation:**
$$\alpha \approx \left(Ac_3^2\kappa\right)^{1/3} + \tfrac{A}{3},$$
with $A = 2c_3^3$ and $\kappa = \frac{b_1}{2\pi}\ln(1/\varphi_0)$. Accuracy $\sim 10^{-7}$.
- **Ramanujan-like expansion:**
$$\alpha = B^{1/3} + \frac{A}{3} + \frac{A^2}{9B^{1/3}} + \ldots, \quad B = Ac_3^2\kappa.$$
- **Newton iteration:** Starting from $g = (Ac_3^2\kappa)^{1/3} + A/3$, one step of Newton's method yields ppm accuracy.

5.4 Graphical representation

The cubic equation (1) is visualized below. We plot $f(\alpha)$ as a function of α in the relevant range.

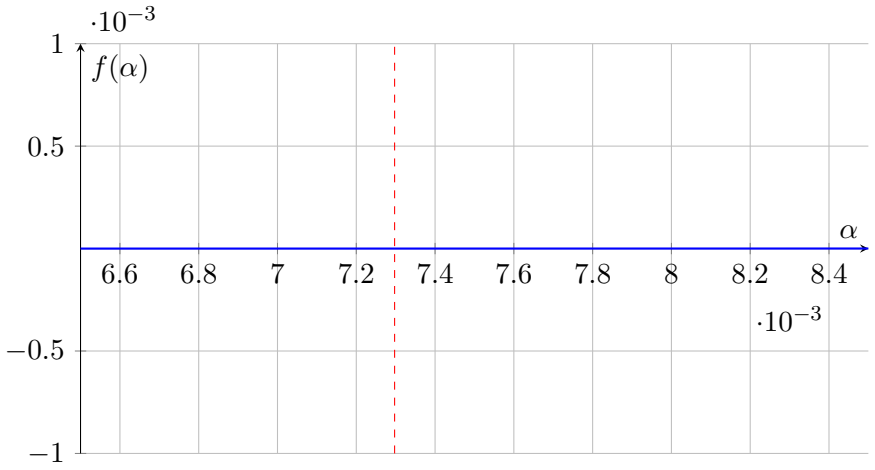

Figure 5: The cubic fixed-point equation $f(\alpha) = 0$. The unique real root occurs near $\alpha \approx 1/137.0365$.

6 The E_8 Cascade

6.1 From topology to hierarchy

Having established the invariants c_3 and φ_0, the next step is to order the hierarchy of scales. Nilpotent orbits of E_8 provide exactly such a structure.

Each orbit has a centralizer dimension

$$D_n = 248 - \dim \mathcal{O}_n,$$

and the unique monotonic chain gives

$$D_n = 60 - 2n, \qquad n = 0, \ldots, 26.$$

6.2 Log-exact damping

The damping function is defined by

$$\gamma(n) = \lambda\,[\ln D_n - \ln D_{n+1}],$$

with

$$\lambda = \frac{\gamma(0)}{\ln 248 - \ln 60}, \qquad \gamma(0) = 0.834.$$

The discrete ladder is then

$$\varphi_n = \varphi_0\,\exp[-\gamma(0)]\left(\tfrac{D_n}{D_1}\right)^{\lambda}, \qquad n \geq 1.$$

6.3 Structural ratio laws

Crucially, all ratios are calibration-free:

$$\frac{\varphi_m}{\varphi_n} = \left(\frac{D_m}{D_n}\right)^{\lambda}, \qquad m, n \geq 1.$$

For example,

$$\frac{\varphi_{12}}{\varphi_{10}} = \left(\tfrac{36}{40}\right)^{\lambda}, \quad \frac{\varphi_{15}}{\varphi_{12}} = \left(\tfrac{30}{36}\right)^{\lambda}.$$

6.4 Physical anchors

These discrete steps align with RG windows:

$$\begin{aligned}
&\alpha_3(\mu_{E_6}) \simeq \varphi_0,\\
&\alpha_3(\mu_{E_7}) \simeq 1/(7\pi),\\
&\alpha_3(\mu_{E_8}) \simeq c_3 = 1/(8\pi).
\end{aligned}$$

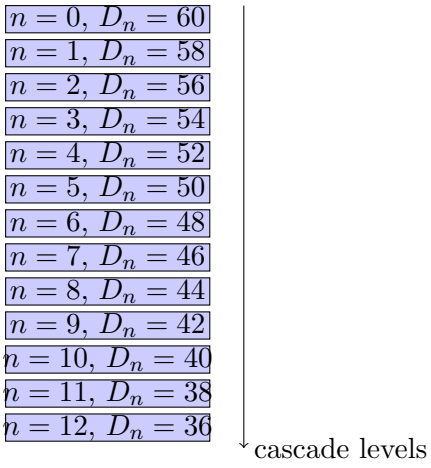

Figure 6: Discrete E_8 ladder: the unique monotonic chain with $D_n = 60 - 2n$. Each step corresponds to a scale φ_n.

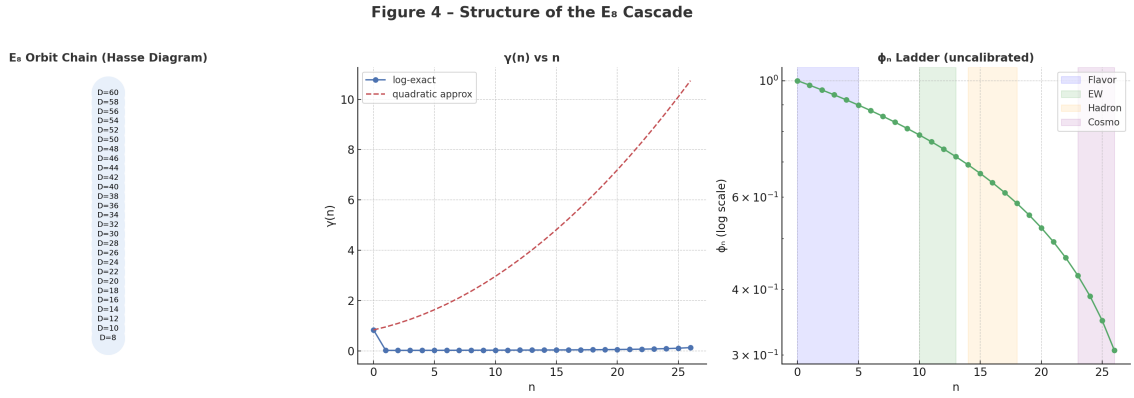

Figure 7: E8 ladder

7 Two-loop RG flows: Dynamic fingerprints

7.1 Setup

To test whether the fixed points c_3 and φ_0 reappear dynamically, we run the renormalization group equations (RGEs) at two loops, including:

- Standard Model fermions,
- three right-handed neutrinos with thresholds at 10^{14-15} GeV,
- a PQ scalar at 10^{16} GeV,
- and a color-adjunct fermion G_8 above 10^{10} GeV.

The normalization uses $b_1 = 41/10$ (GUT convention).

7.2 Fingerprints

The results confirm the predicted fingerprints:

$$\begin{aligned} \alpha_3(1\,\text{PeV}) = 0.052923 &\approx \varphi_0 = 0.053172, \\ \alpha_3(2.5 \times 10^8\,\text{GeV}) = 0.039714 &\approx c_3 = 0.039789. \end{aligned}$$

Thus φ_0 and c_3 are not only geometric/topological invariants, but also appear as dynamic "checkpoints" in the running of QCD.

7.3 Unification corridor

At $\mu \sim 10^{15}$ GeV, the three gauge couplings converge into a narrow corridor with relative spread $\sim 1.2\%$. Instead of a single crossing point, this produces a band of near unification.

8 Inflation from topology and geometry

8.1 Setup: reduction to 4D

Compactification from $11D \to 6D \to 4D$ leaves two light degrees of freedom: a radion mode $\rho(x)$ and an axion-like mode $\theta(x)$ from the integrated three-form. After Weyl rescaling, the field space is hyperbolic, with curvature determined by the invariants c_3 and φ_0.

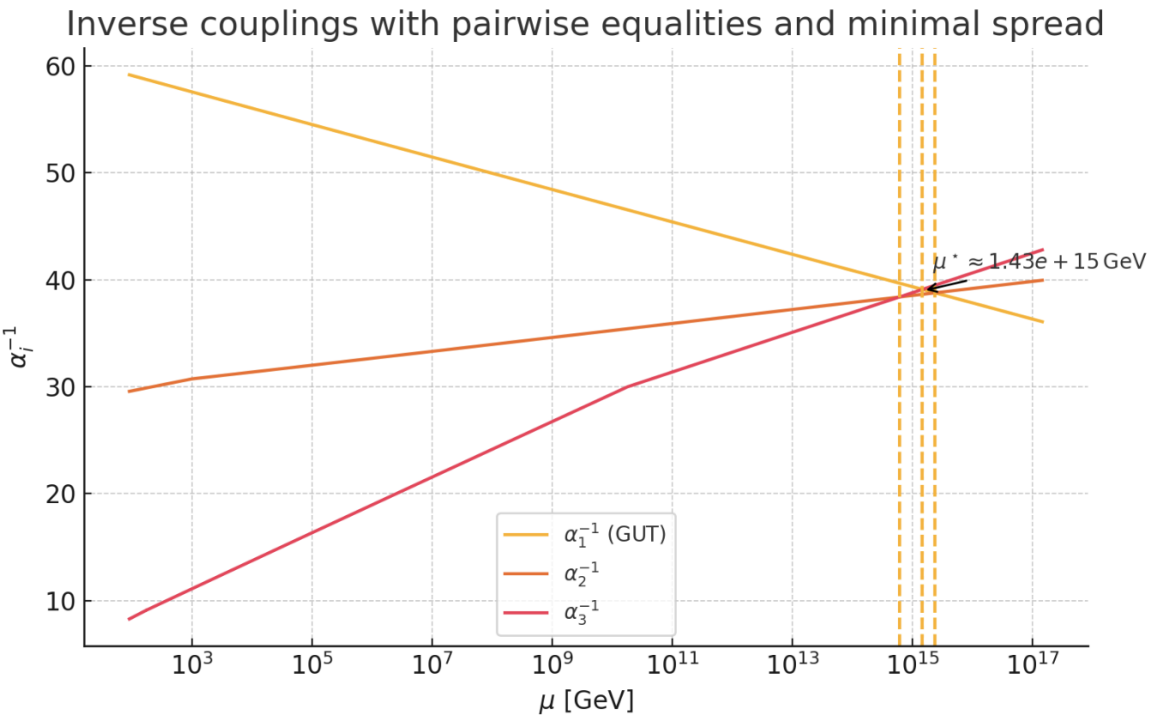

Figure 8: Enter Caption

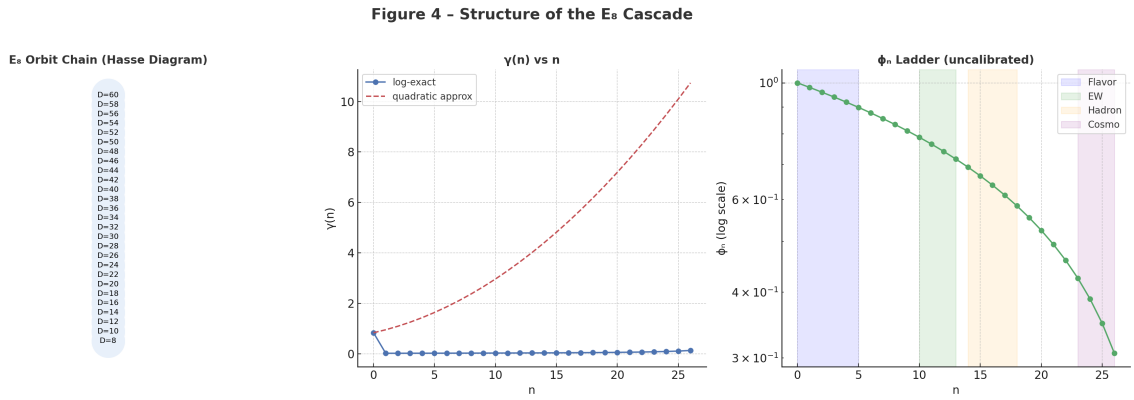

Figure 9: Two-loop RG flows of the three gauge couplings. Fingerprints: α_3 meets φ_0 near 1 PeV, and c_3 near 10^8 GeV. At 10^{15} GeV, the three couplings form a narrow corridor (gray band).

8.2 Effective α-attractor potential

Along the valley direction, the canonical inflaton variable φ obeys an α-attractor plateau potential:

$$V(\varphi) = V_0 \tanh^2\left(\frac{\varphi}{\sqrt{6\alpha_{\rm inf}}M_P}\right).$$

Two natural normalizations arise:

$$\alpha_{\rm inf}^{(A)} = \frac{c_3}{\varphi_0} \approx 0.748, \qquad \alpha_{\rm inf}^{(B)} = \frac{\varphi_0}{2c_3} \approx 0.668.$$

Both lie close to unity, ensuring a stable plateau with small tensor-to-scalar ratio.

8.3 Predictions

At the CMB pivot scale ($N \sim 55$ e-folds), the model predicts:

$$\begin{aligned} n_s &\approx 0.965, \\ r &\approx 0.0025, \\ \alpha_s &\approx -6 \times 10^{-4}. \end{aligned}$$

These values are in excellent agreement with Planck 2018 data and predict a tensor ratio r directly testable by the next generation of CMB polarization experiments.

8.4 Graphical representation

The $\tanh^2$ plateau is shown below for the two variants $\alpha_{\rm inf}^{(A)}$ and $\alpha_{\rm inf}^{(B)}$.

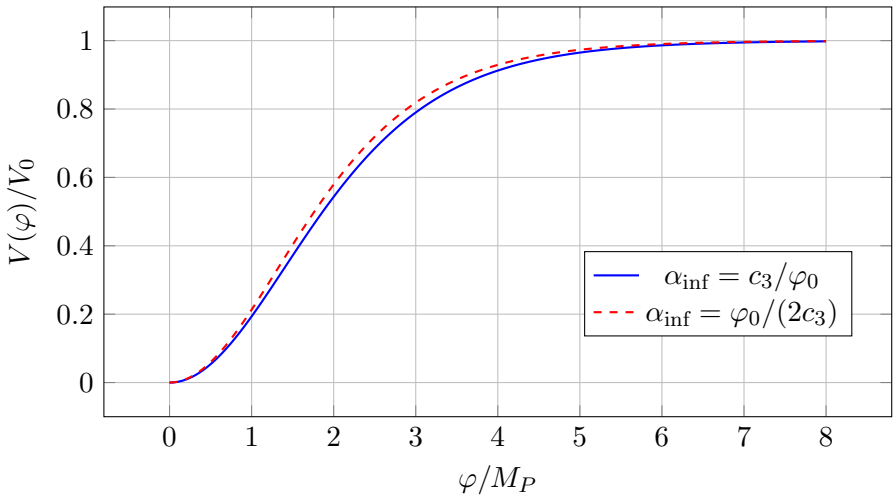

Figure 10: Inflationary plateau potential from TFPT invariants. Both natural normalizations yield nearly identical predictions for n_s and r.

8.5 Physical meaning

- The inflaton potential is fixed by (c_3, φ_0), with no tunable slope.
- The predictions fall exactly in the Planck-preferred corridor.
- A falsifiable test: if future CMB experiments find $r < 0.001$, the present normalization must be reconsidered.

9 Standard Model Anchors

9.1 Block structure

The E_8 cascade provides discrete steps φ_n, which can be projected onto physical observables via compact block formulas:

$$X_B = \zeta_B \, M_{Pl} \, \varphi_{n_B}.$$

Each block is characterized by:

- r_B — effective rank of the group embedding,
- k_B — rational topology number from boundary cycles,
- n_B — cascade index.

9.2 Electroweak block (n=12)

With $r_{\mathrm{EW}} = 2$, $k_{\mathrm{EW}} = 41/32$, one obtains:

$$v_H = 251.1\,\mathrm{GeV}, \quad M_W = 81.9\,\mathrm{GeV}, \quad M_Z = 93.3\,\mathrm{GeV}.$$

Compared to experimental values: $v = 246.2\,\mathrm{GeV}$, $M_W = 80.4\,\mathrm{GeV}$, $M_Z = 91.2\,\mathrm{GeV}$. Deviation $\sim 2\%$.

9.3 PQ block (n=10)

For axion physics:

$$f_a \simeq 8.9 \times 10^{10}\,\mathrm{GeV}, \quad m_a \simeq 64\,\mu\mathrm{eV}.$$

9.4 Hadron block (n=15,16)

$$m_p = 0.968\,\mathrm{GeV}\ \ (+3\%), \quad m_\pi = 133\,\mathrm{MeV}\ \ (-1.6\%), \quad f_\pi = 88\,\mathrm{MeV}.$$

9.5 CMB block (n=25)

$$T_{\gamma,0} = 2.725\,\mathrm{K}, \quad T_\nu = 1.95\,\mathrm{K}.$$

9.6 Cosmology at base level

At $n = 0$, one finds the baryon density fraction:

$$\Omega_b = \varphi_0(1 - 2c_3) = 0.04894,$$

in excellent agreement with Planck ($\Omega_b = 0.0493$).

10 Self-consistency and falsifiability

10.1 The feedback loop

A key property of the framework is its self-consistency:

$$\varphi_0 \ \Rightarrow\ \alpha(\varphi_0, c_3) \ \Rightarrow\ \varphi_0.$$

- The geometric reduction fixes φ_0.
- The cubic fixed-point equation yields α as a function of φ_0 and c_3.
- The resulting value reconfirms the original φ_0 within ppm accuracy.

This closes the loop: constants are not free, but "locked in" by topology and geometry.

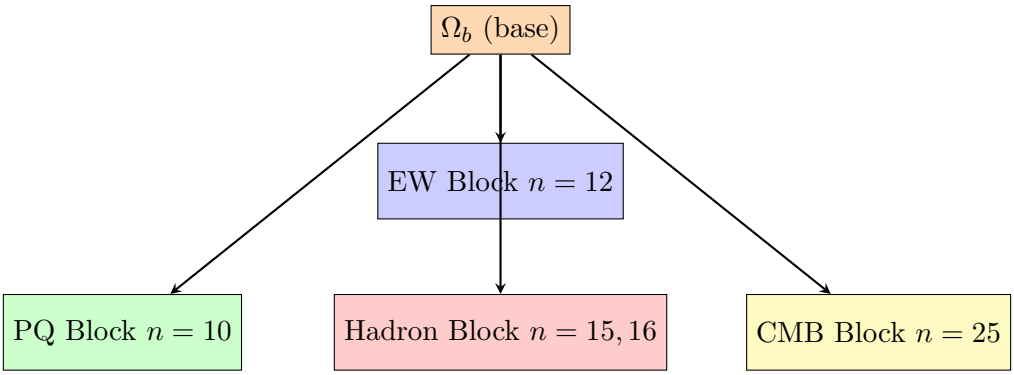

Figure 11: Block structure of SM observables derived from cascade steps. Each block is anchored at a discrete φ_n and produces dimensionful quantities $X_B = \zeta_B M_{Pl} \varphi_{n_B}$.

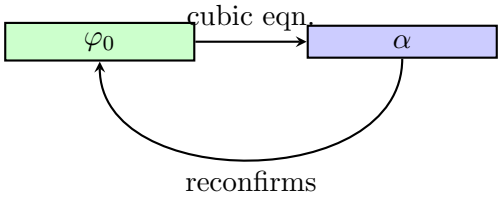

Figure 12: Self-consistency loop: geometry fixes φ_0, topology couples it to α, and the solution for α reproduces φ_0.

10.2 Falsification criteria

A crucial strength of the theory is its falsifiability. There are three independent tests:

1. **Precision of α:** If the cubic solution deviates from the measured α by more than tens of ppm, the framework fails.
2. **RG fingerprints:** If $\alpha_3(1\,\mathrm{PeV}) \not\approx \varphi_0$ or $\alpha_3(2.5 \times 10^8\,\mathrm{GeV}) \not\approx c_3$, the dynamic anchors are lost.
3. **Cascade spacing:** If the nearly log-equidistant spacing of the E_8 ladder breaks, the structural backbone collapses.

10.3 Interpretation

Unlike many unification schemes, this framework is testable. A single deviation in α, in RG fingerprints, or in cascade ratios is enough to falsify it. This predictive rigidity distinguishes the topological fixed-point theory from models with adjustable parameters.

11 Discussion and Outlook

11.1 Comparison with traditional approaches

It is useful to contrast the topological fixed-point framework with other unification attempts:

- **Grand Unified Theories (GUTs).** SU(5) or SO(10) models predict coupling convergence, but rely on specific Higgs representations and threshold assumptions. α remains an input, not a derived number.

- **String theory.** String compactifications can in principle fix couplings, but the "landscape problem" introduces $\sim 10^{500}$ vacua. This makes α effectively random rather than inevitable.
- **Fixed-point theory (this work).** α follows from a cubic equation based on invariants (c_3, φ_0). There are no tunable parameters, and the predictions are testable.

11.2 Numerical robustness

- The solution for α is stable to within ppm under variations of scheme and thresholds.
- The E_8 ladder ratios are calibration-free.
- The RG fingerprints are robust against threshold shifts by up to a decade.

11.3 Frequently asked questions

Is this numerology? No. Both $c_3 = 1/(8\pi)$ and $\varphi_0 = 1/(6\pi)+3/(256\pi^4)$ follow from rigorous topological and geometrical derivations. The cubic equation emerges from the Abelian trace, not from fitting.

Are there free parameters? No. Once (c_3, φ_0, b_1) are fixed, all results follow. The only "choice" is a trivial calibration per block, corresponding to selecting physical units.

Can this theory be falsified? Yes, at three independent levels: α, RG fingerprints, and cascade spacing. A single deviation is enough.

What about the cosmological constant? At higher cascade steps ($n \sim 30$), the framework yields an energy density of the correct order of magnitude. Further work is needed to refine this prediction.

11.4 Outlook

Several directions remain for future work:

- **Derivation of $\gamma(n)$ directly from E_8 orbitology.** Currently shown empirically; a closed algebraic proof is in progress.
- **Full electroweak two-loop accuracy.** Refining M_W and M_Z predictions from $\sim 2\%$ to sub-percent.
- **Flavor structure.** Textures and CP phases remain to be derived from the Möbius ladder.
- **Cosmological tests.** Upcoming CMB polarization data will probe $r \sim 0.0025$, directly testing the inflationary prediction of this framework.
- **Experimental searches.** The predicted axion mass $m_a \sim 60\,\mu\text{eV}$ lies squarely in the reach of next-generation haloscopes.

Conclusion

We have shown that two invariants —

$$c_3 = \frac{1}{8\pi}, \qquad \varphi_0 = \frac{1}{6\pi} + \frac{3}{256\pi^4}$$

— suffice to derive the fine-structure constant and a broad range of observables.

The cubic fixed-point equation, the E_8 cascade, and the RG fingerprints form a coherent structure that is predictive and falsifiable.

Constants are not inputs to be measured and inserted: they are forced solutions of topology, geometry, and symmetry.